Extremely nondegenerate two-photon absorption in direct-gap semiconductors [Invited]

Claudiu M. Cirloganu, Lazaro A. Padilha, Dmitry A. Fishman, Scott Webster, David J. Hagan, and Eric W. Van Stryland*

CREOL: The College of Optics and Photonics, University of Central Florida, 4000 Central Florida Blvd, Orlando, FL, 32816, USA

**ewvs@creol.ucf.edu*

Abstract: Two-photon absorption (2PA) spectra with pairs of extremely nondegenerate photons are measured in several direct-gap semiconductors (GaAs, CdTe, ZnO, ZnS and ZnSe) using picosecond or femtosecond pulses. In ZnSe, using photons with a ratio of energies of ~12, we obtain a 270-fold enhancement of 2PA when comparing to the corresponding degenerate 2PA coefficient at the average photon energy $(\eta\omega_1 + \eta\omega_2)/2$. This corresponds to a pump photon energy of 8% of the bandgap. 2PA coefficients as large as 1 cm/MW are measured. Thus, by using two widely different wavelengths we are able to access the large 2PA observed previously only in narrow gap semiconductors. We also calculate the corresponding enhancement of nonlinear refraction, consisting of two-photon, AC-Stark and Raman contributions. The net effect is a smaller enhancement, but exhibits very large dispersion within the 2PA regime.

OCIS codes: (190.0190) Nonlinear optics; (300.6410) Spectroscopy, multiphoton; (190.7110) Ultrafast nonlinear optics.

References and links

1. J. A. Bolger, A. K. Kar, B. S. Wherrett, R. DeSalvo, D. C. Hutchings, and D. J. Hagan, "Nondegenerate two-photon absorption spectra of ZnSe, ZnS and ZnO," Opt. Commun. **97**(3–4), 203–209 (1993).
2. A. A. Said, M. Sheik-Bahae, D. J. Hagan, T. H. Wei, J. Wang, J. Young, and E. W. Van Stryland, "Determination of bound-electronic and free-carrier nonlinearities in ZnSe, GaAs, CdTe, and ZnTe," J. Opt. Soc. Am. B **9**(3), 405–414 (1992).
3. M. Sheik-Bahae, D. C. Hutchings, D. J. Hagan, and E. W. Van Stryland, "Dispersion of bound electron nonlinear refraction in solids," IEEE J. Quantum Electron. **27**(6), 1296–1309 (1991).
4. E. W. Van Stryland, M. A. Woodall, H. Vanherzeele, and M. J. Soileau, "Energy band-gap dependence of two-photon absorption," Opt. Lett. **10**(10), 490–492 (1985).
5. P. D. Olszak, C. M. Cirloganu, S. Webster, L. A. Padilha, S. Guha, L. P. Gonzalez, S. Krishnamurthy, D. J. Hagan, and E. W. Van Stryland, "Spectral and temperature dependence of two-photon and free-carrier absorption in InSb," Phys. Rev. B **82**(23), 235207 (2010).
6. B. S. Wherrett, "Scaling rules for multiphoton interband absorption in semiconductors," J. Opt. Soc. Am. B **1**(1), 67–72 (1984).
7. D. A. Fishman, C. M. Cirloganu, S. Webster, L. A. Padilha, M. Monroe, D. J. Hagan, and E. W. Van Stryland, "Sensitive mid-infrared detection in wide-gap semiconductors using extreme nondegenerate two-photon absorption," Nat. Photonics **5**(9), 561–565 (2011).
8. F. Urbach, "The long-wavelength edge of photographic sensitivity and of the electronic absorption of solids," Phys. Rev. **92**(5), 1324 (1953).
9. A. E. Rakhshani, "Study of Urbach tail, bandgap energy and grain-boundary characteristics in CdS by modulated photocurrent spectroscopy," J. Phys. Condens. Matter **12**(19), 4391–4400 (2000).
10. S. Keuleyan, E. Lhuillier, V. Brajuskovic, and P. Guyot-Sionnest, "Mid-infrared HgTe colloidal quantum dot photodetectors," Nat. Photonics **5**(8), 489–493 (2011).
11. A. Hayat, P. Ginzburg, and M. Orenstein, "Observation of two-photon emission from semiconductors," Nat. Photonics **2**(4), 238–241 (2008).
12. D. C. Hutchings, M. Sheik-Bahae, D. J. Hagan, and E. W. Stryland, "Kramers-Kronig Relations in Nonlinear Optics," Opt. Quantum Electron. **24**(1), 1–30 (1992).
13. F. T. Arecchi, E. O. Schulz-Dubois, M. L. Stitch, W. B. Colson, C. Pellegrini, and A. Renieri, Laser handbook. 1972, Amsterdam, New York: North-Holland Pub. Co.; American Elsevier Pub. Co. v. <1–6 >.

#153971 - $15.00 USD Received 6 Sep 2011; revised 24 Oct 2011; accepted 25 Oct 2011; published 28 Oct 2011

14. A. Bhaskar, G. Ramakrishna, Z. Lu, R. Twieg, J. M. Hales, D. J. Hagan, E. Van Stryland, and T. Goodson 3rd, "Investigation of two-photon absorption properties in branched alkene and alkyne chromophores," J. Am. Chem. Soc. **128**(36), 11840–11849 (2006).
15. D. C. Hutchings and E. W. V. Stryland, "Nondegenerate two-photon absorption in zinc blende semiconductors," J. Opt. Soc. Am. B **9**(11), 2065–2074 (1992).
16. J. M. Hales, D. J. Hagan, E. W. Van Stryland, K. J. Schafer, A. R. Morales, K. D. Belfield, P. Pacher, O. Kwon, E. Zojer, and J. L. Bredas, "Resonant enhancement of two-photon absorption in substituted fluorene molecules," J. Chem. Phys. **121**(7), 3152–3160 (2004).
17. H. D. Jones and H. R. Reiss, "Intense-field effects in solids," Phys. Rev. B **16**(6), 2466–2473 (1977).
18. D. C. Hutchings and B. S. Wherrett, "Theory of anisotropy of 2-photon absorption in zincblende semiconductors," Phys. Rev. B **49**(4), 2418–2426 (1994).
19. C. M. Cirloganu, P. D. Olszak, L. A. Padilha, S. Webster, D. J. Hagan, and E. W. V. Stryland, "Three-photon absorption spectra of zinc blende semiconductors: theory and experiment," Opt. Lett. **33**(22), 2626–2628 (2008).
20. L. V. Keldysh, "Ionization in field of a strong electromagnetic wave," Soviet Phys. JETP **20**(5), 1307 (1965).
21. H. S. Brandi and C. B. Dearaujo, "Multiphoton absorption-coefficients in solids – a universal curve," J. Phys. C Solid State Phys. **16**(30), 5929–5936 (1983).
22. M. Balu, L. Padilha, D. Hagan, E. Van Stryland, S. Yao, K. Belfield, S. Zheng, S. Barlow, and S. Marder, "Broadband Z-scan characterization using a high-spectral-irradiance, high-quality supercontinuum: erratum," J. Opt. Soc. Am. B **26**(8), 1663–1663 (2009).
23. R. A. Negres, J. M. Hales, D. J. Hagan, and E. W. Van Stryland, "Experiment and analysis of two-photon absorption spectroscopy using a white-light continuum probe," IEEE J. Quantum Electron. **38**(9), 1205–1216 (2002).
24. M. Balu, L. A. Padilha, D. J. Hagan, E. W. Van Stryland, S. Yao, K. Belfield, S. Zheng, S. Barlow, and S. Marder, "Broadband Z-scan characterization using a high-spectral-irradiance, high-quality supercontinuum," J. Opt. Soc. Am. B **25**(2), 159–165 (2008).
25. M. Sheik-Bahae, A. A. Said, T. H. Wei, D. J. Hagan, and E. W. Van Stryland, "Sensitive measurement of optical nonlinearities using a single beam," IEEE J. Quantum Electron. **26**(4), 760–769 (1990).
26. K. Ikeda and Y. Fainman, "Material and structural criteria for ultra-fast Kerr nonlinear switching in optical resonant cavities," Solid-State Electron. **51**(10), 1376–1380 (2007).
27. C. N. Ironside, "2-Photon Gain Semiconductor Amplifier," IEEE J. Quantum Electron. **28**(4), 842–847 (1992).

1. Introduction

The two-photon absorption (2PA) processes in semiconductors have been extensively studied both experimentally and theoretically, resulting in what are now well-established scaling rules that can accurately predict the degenerate two-photon absorption (D-2PA) of direct-gap semiconductors [1-3]. These scaling rules show that D-2PA is inversely proportional to the cube of the energy gap, E_g. This means that the D-2PA coefficients in narrow-gap semiconductors are two to three orders of magnitude greater than the absorption than in large-gap semiconductors. For example, ZnO (E_g = 3.2eV) has a D-2PA two-photon absorption coefficient, $\alpha_2 \approx 5$ cm/GW at 532 nm [4], while for InSb (E_g = 0.23eV), $\alpha_2 \approx 2$ cm/MW in the range 8 to 12 μm [5]. 2PA coefficients in the cm/MW range may prove useful for practical applications, but these scaling rules imply that such large values are not accessible in the near infrared (NIR)/visible (VIS) range. For non-degenerate two-photon absorption (ND-2PA), the energies of individual photons may approach intermediate-state resonances that allow the 2PA to become much larger than in the degenerate case. As is well known, in the case of 2PA for a two-band model, the dominant transitions are either inter-band ("direct/allowed") or intra-band "self/forbidden" [6]. This suggests that such intermediate state resonances can become significant only when using photons with energies either very small or approaching the bandgap energy, such that the two photons employed in the process would have extremely different energies. We recently presented results of extremely ND-2PA (END-2PA) in ZnSe and GaAs and its application to gated infrared detection using a GaN-based detector [7]. In this current work, we report on more extensive studies including several other semiconductors along with theoretical calculations showing that END-2PA can exceed their degenerate counterparts by two to three orders of magnitude. We consider END-2PA as a non-degenerate process where the possible "intermediate" states lie energetically very close to both the initial state (in the valence band) or the final state (in the conduction band). This generally implies that the lower energy photon is much less than half the bandgap, placing it in the mid-infrared (MIR) when the semiconductors have visible or NIR bandgaps. As the lower energy photon

#153971 - $15.00 USD Received 6 Sep 2011; revised 24 Oct 2011; accepted 25 Oct 2011; published 28 Oct 2011

moves further into the IR significant enhancements will be realized, but, may be influenced by thermal broadening of the Urbach tail due to electron/exciton phonon interaction [8,9]. This allows the extremely large 2PA coefficients, previously only seen in narrow-gap semiconductors, to be observed in larger-gap semiconductors such as CdTe, GaAs, ZnSe, ZnO, and ZnS. The large enhancement of 2PA can be useful for optical switching, infrared (IR) detection [10] and could have important consequences for lasers and amplifiers based on two-photon gain [11]. Making use of our previous work using Kramers-Kronig relations to obtain the dispersion of the nonlinear refraction [3,12], we also predict an enhancement of the non-degenerate nonlinear refractive index n_2; however, positive and negative contributions from the two-photon, Raman and AC-Stark terms lead to a smaller enhancement but an extremely rapid dispersion in the 2PA region.

2. Theoretical background

While data for ND-2PA exist from the earliest experimental papers [13], besides our recent results [6], no other data exist to our knowledge with a ratio of photon energies larger than 3.3 [14]. As seen from Eq. (1) this is an interesting realm to investigate since as the intermediate state for the transition approaches an eigenstate of the system, the 2PA is expected to diverge (of course adding in decay insures overall convergence). In the case of END-2PA there are two resonances that can be exploited. As predicted by Wherrett [6] and verified in Ref [4], the allowed-forbidden transitions dominate 2PA in direct-gap semiconductors so that the small energy photon can become near resonant to the "forbidden" or self-transition while the large energy photon can be nearly bandgap resonant. This is illustrated in Fig. 1, and may be easily seen qualitatively from the expression for the ND-2PA rate, W_2^{ND}, which can be written in the perturbative framework [15] as

$$W_2^{ND} = \frac{2\pi}{\hbar}\sum_{vc}\left|\sum_i\left[\frac{\langle c|H_2|i\rangle\langle i|H_1|v\rangle}{E_{iv}(\mathbf{k})-\hbar\omega_1}+\frac{\langle c|H_1|i\rangle\langle i|H_2|v\rangle}{E_{iv}(\mathbf{k})-\hbar\omega_2}\right]\right|^2\delta\left[E_{cv}(\mathbf{k})-\hbar\omega_1-\hbar\omega_2\right] \quad (1)$$

with indices *1* and *2* designating the two photons, *H* the electron-field interaction Hamiltonian and *v*, *c* and *i* the valence, conduction and intermediate states, respectively.

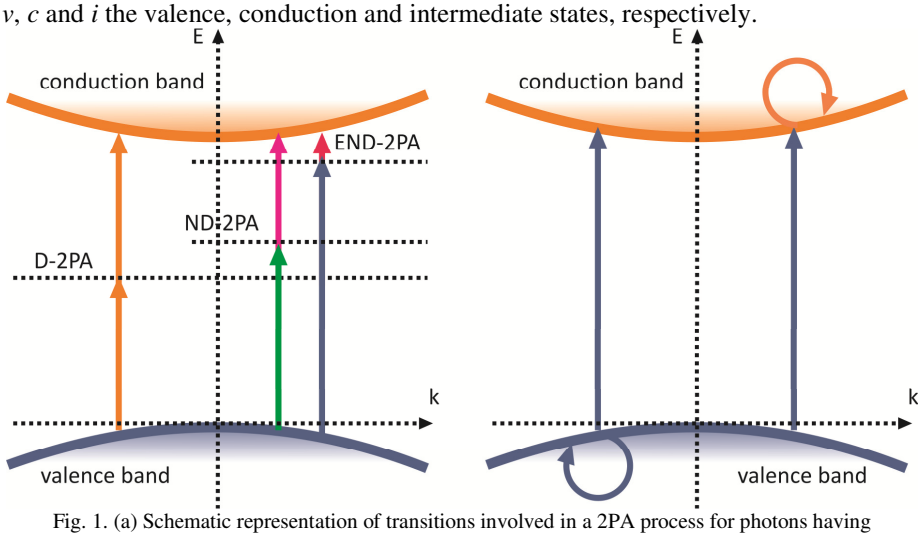

Fig. 1. (a) Schematic representation of transitions involved in a 2PA process for photons having various energy ratios, with ND-2PA and END-2PA characterized by a small detuning energy as compared to the bandgap. (b) The equivalent representation within the perturbative framework showing the possible transitions for two-band structure consisting of direct ("allowed") and self ("forbidden") transitions.

#153971 - $15.00 USD Received 6 Sep 2011; revised 24 Oct 2011; accepted 25 Oct 2011; published 28 Oct 2011

If one considers the simple model of a two-band direct-gap semiconductor, the virtual state can be taken as either the initial (in the valence band) or the final state (in the conduction band) for the electron transition, in which case one resonance occurs for both the low and high-energy photons (see Fig. 1b). For this case, since E_{iv} is either equal to 0 or to $E_{cv} = \hbar\omega_1 + \hbar\omega_2$, one can write explicitly the contributions from different paths of evolution for the system and obtain

$$W_2^{ND} \sim \left| \frac{M_{vc}^2 M_{vv}^1}{-\hbar\omega_1} + \frac{M_{vc}^1 M_{vv}^2}{-\hbar\omega_2} + \frac{M_{cc}^2 M_{vc}^1}{\hbar\omega_2} + \frac{M_{cc}^1 M_{vc}^2}{\hbar\omega_1} \right|^2, \tag{2}$$

where $M_{ij}^{1,2} = \langle j | H_{1,2} | i \rangle$ are the corresponding matrix elements. The matrix elements are linear in the amplitude of the magnetic vector potential associated with the respective fields, which in turn are expressed in terms of ratios of square root of irradiances divided by photon energies. Overall, taking also into account the expression of non-degenerate 2PA $\alpha_2(\omega_1;\omega_2) = \hbar\omega_1 W_2^{ND} / (I_1 I_2)$, we obtain a complex and stronger dependence on the photon energies of the interacting fields as exemplified below with the functional form of 2PA as derived in Ref [3]. Smaller photon energies will decrease the denominator values thus increasing the 2PA. It is important to observe here that each of the two different possible transition sequences yields a term enhanced significantly by the presence of a small energy photon. This effect is similar to the intermediate state resonance enhancement (ISRE) predicted and seen in molecular systems [14,16]. In direct-gap semiconductors the one-photon absorption (1PA) edges are generally sharper than those of organics and therefore larger enhancements may be obtained when probing very close to the linear absorption range.

Theoretical calculations of third-order nonlinearities in semiconductors are very well documented, and there are a couple of approaches commonly used in the past. One of the methods involves the use of second-order perturbation theory, as in Eq. (1), to directly calculate the transition rates using a quantum mechanical description (eigenvalues and eigenstates) of the considered systems. Reasonable predictions can be made either using a simple two-parabolic band model [6,17] or one can employ complex 4- or 7-band calculations for better accuracy, which can go as far as predicting the anisotropy of the nonlinear coefficients for particular systems like the ones exhibiting zinc-blende symmetry [15,18]. The 2PA spectra obtained with these models are similar as more complex numerical calculations only lead to shifts in the magnitudes of the coefficients producing minor changes to the spectral shapes [15]. This is quite different from the case of three-photon absorption (3PA) where different pathways result in quantum interference leading to very different results depending on the band model used [19]. Another theoretical method that was successfully used in the past and in the calculations shown in this paper, is based on Keldysh's tunneling theory [20]. It uses a scattering matrix formalism with Volkov-type "dressed" wavefunctions for the electronic states in order to account for the effect of the electric field on the system [3,17,21]. This provides similar 2PA spectra to the perturbation methods and yields identical results for the simple case of two-parabolic bands and D-2PA. As shown in Ref [3], the ND-2PA coefficient $\alpha_2(\omega_1;\omega_2)$ is calculated in this scattering matrix formalism with two parabolic bands to be:

$$\alpha_2(\omega_1;\omega_2) = K \frac{\sqrt{E_p}}{n_1 n_2 E_g^{\,3}} F_2\left(\frac{\hbar\omega_1}{E_g};\frac{\hbar\omega_2}{E_g}\right),$$

$$where \quad F_2(x_1;x_2) = \frac{(x_1 + x_2 - 1)^{3/2}}{2^7 x_1 x_2^2}\left(\frac{1}{x_1} + \frac{1}{x_2}\right)^2, \tag{3}$$

#153971 - $15.00 USD Received 6 Sep 2011; revised 24 Oct 2011; accepted 25 Oct 2011; published 28 Oct 2011

for the optical frequencies $\omega_{1,2}$, E_p is the Kane energy parameter, E_g is the bandgap energy, $n_{1,2}$ *are* the refractive indices, and K is a material independent parameter. We should mention here that a similar expression is obtained using the perturbation approach as shown in [15] (see Eqs. (15) and 16).

3. Experimental results

The experimental ND-2PA spectra presented in this paper are taken in a standard pump-probe non-collinear geometry with a small angle (~7 degrees) between the pump and the probe beams, using either picosecond or femtosecond pulses. The temporal scans are obtained by delaying either the pump (femtosecond data) or the probe (picosecond data) using a retroreflector mounted on a computer-controlled motorized translation stage. The picosecond pump-probe experiments are performed using a 10Hz EKSPLA laser system (PL-2143C). It consists of a ~30 ps FWHM modelocked Nd:YAG 1064 nm laser, converted to the third harmonic at 355 nm and pumping two LBO-based optical parametric generation/amplification (OPG/OPA) devices. The IR pump beam for our experiments is obtained through a difference frequency generation (DFG) process in a GaSe crystal using 1064 nm from the laser and the idler beam from a second similar OPG/OPA system. The IR pumping wavelength is chosen to be 8840 nm corresponding to approximately 10% of the bandgap of GaAs, which together with CdTe are the two semiconductors studied in this configuration. Our choice of pump wavelength is also based on the available tuning range of the IR (8-14 μm) and taking into account the energy and beam quality at the output wavelengths. The probe beam is selected by tuning the idler output to individual wavelengths in the near-IR. Our probe beam has a maximum energy of a few nJs and a smaller spot size than that of the pump, as measured by knife-edge scans, with a ratio of 1:2. This assures an irradiance in the probe beam smaller by at least a factor of 100 than the pump beam irradiance. In our configuration, this causes minimal losses through D-2PA of the probe (< 0.5%, which is at our noise level).

A similar setup is used for our femtosecond experiments. The system consists of a 1 kHz Clark MXR Ti:Sapphire laser pumping two BBO- based TOPAS OPG/OPA systems from Light Conversion Inc. with an infrared beam obtained through DFG in a $AgGaS_2$ crystal, like in the case of the picoseconds system. The pump used for these experiments is in the wavelength range of 1200 nm to 5600 nm, corresponding to approximately 30% to 8% of the bandgap energy for the semiconductors studied (ZnSe, ZnS, ZnO). Depending on wavelength, it can be either the idler output of the TOPAS or obtained through DFG. Autocorrelation measurements of the pulsewidths yield values of ~140 fs FWHM. The probe is obtained from a white-light continuum (WLC) generated using the 1300 nm signal beam from the TOPAS into a 2 mm thick piece of CaF_2. Individual wavelengths are selected from the WLC using a set of interference filters with a spectral bandwidth of ~10 nm. The temporal width of the spectrally filtered pulses is between 140 fs and 160 fs as verified by autocorrelation experiments [22]. The pump to probe spot size ratio is ~7 to 1 giving a minimum ratio for the pump to probe irradiance of 20. Similar to the picoseconds experiments, the probe energy is small enough that any self-induced probe beam 2PA can be neglected.

In all our nondegenerate experiments, the pump or excitation beam (I_e), is always at the longer wavelength, with photon energies less than a third of the bandgap. This is to avoid any 2PA or 3PA caused by the pump itself which would complicate the experiment and the analysis of the experimental data, and would lead to the creation of free-carrier pairs which would cause extra losses especially for longer pulses. Hence, absorption is solely caused by ND-2PA with one photon being absorbed from each beam. Although this absorption also produces free carriers, the density of carriers produced is proportional to the photon density from the weak probe beam which is deliberately kept very small. For our experiments, effects of free-carrier absorption and refraction can be ignored altogether. Thus, the irradiance dependent pump-probe results are modeled by,

#153971 - $15.00 USD Received 6 Sep 2011; revised 24 Oct 2011; accepted 25 Oct 2011; published 28 Oct 2011

$$\frac{dI_p(\omega_p)}{dz} = -2\alpha_2(\omega_p;\omega_e)I_e(\omega_e)I_p(\omega_p). \quad (4)$$

The second reason the low photon energy beam is used as the pump is related to the magnitude of the 2PA coefficient, which scales with the photon energy at which the absorption is monitored. The frequency dependence of the 2PA coefficient (3) through the F_2 function leads to the relation $\alpha_2(\omega_p;\omega_e)/\alpha_2(\omega_e;\omega_p) = \omega_p/\omega_e$. This is because the rate of photon loss must be the same for both beams, hence the energy loss rate is larger for the beam with higher energy photons. Because the photon loss rates are identical, the carrier generation rate is symmetric in the two wavelengths. Thus, as noted in [7], the END enhancement in two-photon detection is the same regardless of which wavelength is the signal or the gate.

The use of a low frequency pump allows for the variation of the probe frequency only over a limited range set by the lowest energetically possible transition and the linear absorption edge, i.e. the probe photon energy can be varied between E_g - $\hbar\omega_e$ and E_g. Typical experimental data are shown in Fig. 2 for CdTe with picosecond pulses (a) and ZnO with femtosecond pulses (b). In the picosecond experiments, $\hbar\omega_e$ is approximately 9.3% of the CdTe bandgap. For the case of femtosecond experiments there are more choices for the pump wavelength. In ZnO, for instance, we are able to choose $\hbar\omega_e$ equal to ~32%, 23%, 19.5%, 17% and 15.5% of E_g. The lowest pump energy corresponds to 2.5 μm which is at the end of our femtosecond OPG/OPA tuning range. Using DFG we also used a pump wavelength of 5.6 μm in ZnSe, which corresponds to about 8% of the bandgap energy.

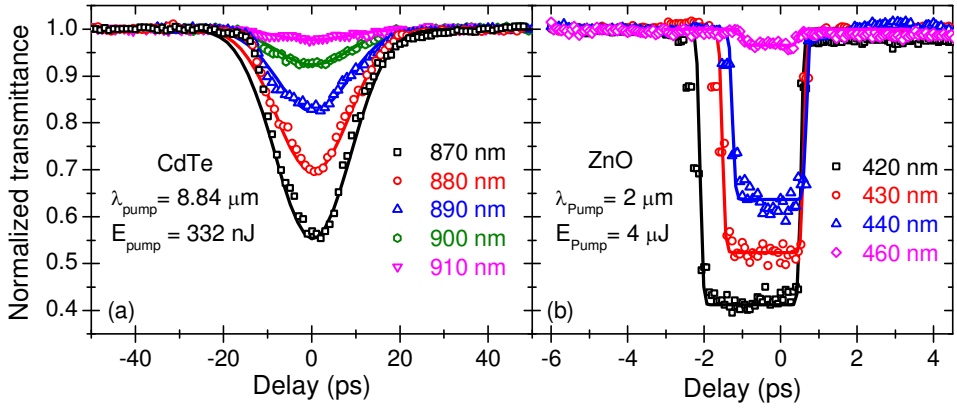

Fig. 2. Typical experimental pump-probe data in CdTe (a) using picoseconds pulses and ZnO (b) using femtosecond pulses along with theoretical fits (solid lines).

For femtosecond pulses, group velocity dispersion (GVD) plays a very important role. This is apparent in the shape of our temporal pump-probe curves as seen in Fig. 2b. Because the group velocity varies strongly with wavelength, for a large range of initial delays, the pump (fast) and probe (slow) walk through each other as they propagate through the sample. The measured effect is a consequence of "effective" temporal overlaps, and as this "effective" overlap distance is smaller than the sample thickness we obtain the same change in transmittance for a range of initial delays. The data were analyzed taking these effects into consideration according to the treatment given in [23]. It should be mentioned that the new femtosecond data shown here is collected without the use of modulation techniques unlike in our previous publication [7].

In Fig. 3 (a) we show the measured END-2PA spectra of GaAs and CdTe along with the calculated curves and plotted versus the average photon energy, thus comparing the coefficients for two transition processes between the same energy levels. This allows convenient representation of the data on the same graph along with the degenerate 2PA

#153971 - $15.00 USD Received 6 Sep 2011; revised 24 Oct 2011; accepted 25 Oct 2011; published 28 Oct 2011

spectrum taken with the femtosecond system using the Z-Scan technique [24]. In all our plots the photon energies are shown scaled to the respective bandgap energies since this allows comparing different semiconductors on the same scale and makes the comparison to the respective degenerate values easier. The theoretical values are represented with solid lines together with measured degenerate data. The measured nondegenerate values are as large as 1 cm/MW, ~180 × larger than the corresponding degenerate values and about 40 × larger than the peak value for the degenerate 2PA. There is a remarkable agreement between the measured and the predicted values using the simple two parabolic-band model over a large range of photon energies. This agreement is not entirely surprising since in experiments with very nondegenerate photons the states involved in transitions are close to the center of the Brillouin zone where the parabolic approximation works best. However, we are able to measure some small signals when the sum of the energies of the two photons falls below the band edge. The analysis shows that the signals are linear in pump energy confirming a ND-2PA process as we are accessing states within the Urbach tail. Due to the large enhancement we are able to measure such small contributions which would otherwise be impossible to do using degenerate photons. Thus END-2PA may be useful for studying the impurity and defect absorption in the Urbach tail.

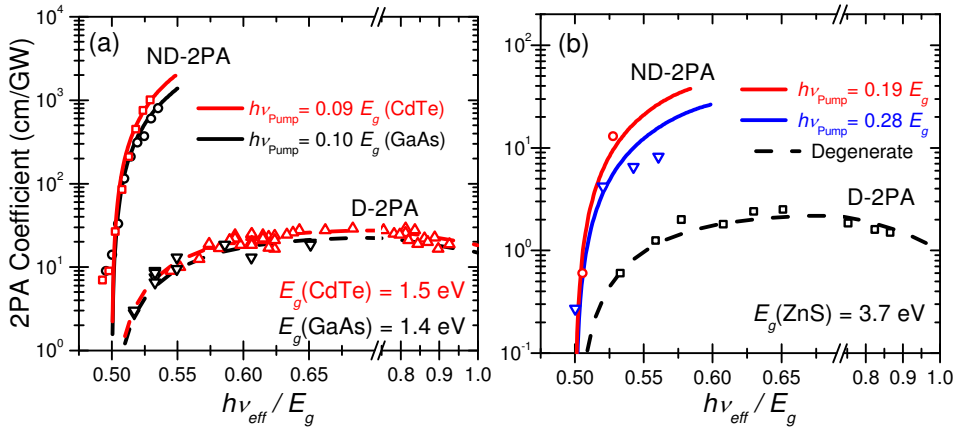

Fig. 3. Non-degenerate 2PA spectra of CdTe and GaAs measured with picosecond pulses (a) and of ZnS measured with femtosecond pulses (b). The theoretically calculated non-degenerate spectra are shown with straight lines, while the dashed lines denote the respective degenerate spectra, along with measured degenerate data. The non-degenerate data in GaAs was taken from [7].

A summary of results obtained using femtosecond pulses is presented in Fig. 3(b) for ZnS and in Fig. 4 for ZnSe (a) and ZnO (b). For these cases the choices of pump and probe photon energies are limited by the specifics of our experimental apparatus. Taking data with small photon energies in the pump beam proved difficult for the largest bandgap semiconductors, since for these cases the probe photons are close to the UV, and in our continuum the energies available for this part of the spectrum are low. The smallest pump photon energy corresponds to approximately 15.5%, 8% and 19% of the bandgap of ZnO, ZnSe and ZnS, respectively. Consequently, the measured maximum enhancement of the nondegenerate values with respect to the degenerate ones varies strongly with the pump photons' energy, reaching ~40 in ZnO and ~270 in ZnSe. As shown, there is again good agreement between theory and femtosecond experimental data. Similarly, the plotted degenerate data was taken using the femtosecond system using the Z-scan technique [25].

#153971 - $15.00 USD Received 6 Sep 2011; revised 24 Oct 2011; accepted 25 Oct 2011; published 28 Oct 2011

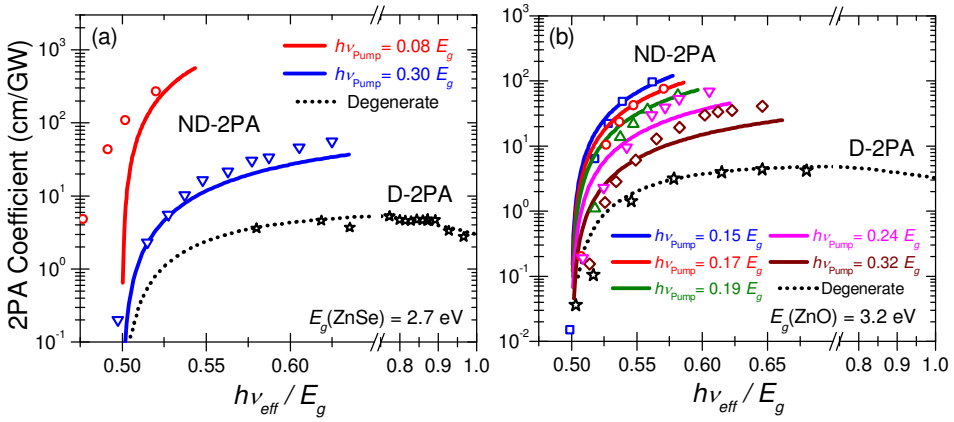

Fig. 4. Non-degenerate 2PA spectra of ZnSe (a) and ZnO (b) measured with femtosecond pulses. The theoretically calculated non-degenerate spectra are shown with straight lines, while the dashed lines denote the respective degenerate spectra, along with measured degenerate data. The 2PA data in (a) was taken from [7] and the degenerate data in (b) was taken from [24].

4. Discussion

The data taken on ZnO best illustrates the strong dependence of the measured values on the pump wavelength. The longer the pump wavelength, the stronger is the enhancement seen in the 2PA. The largest overall magnitude we measure is about 1 cm/MW using the mid-IR pump. We point out here that these nonlinearities are measured at visible and near IR wavelengths and their magnitudes come close to the degenerate values measured in narrow-gap semiconductors (e.g. InSb, InAs, etc.) at wavelengths in the mid-infrared. This can be understood by considering the perturbative expression (Eq. (2) of the 2PA rate when using a simple two-band model for a given pair of initial and final states. For the nondegenerate case, the energy term in the denominator gets as small as the pump energy with one of the two terms being highly enhanced for either of the transition paths possible (a first "self" transition followed by a direct transition or vice versa) as is written in Eq. (5) .

$$W_2^{\,D} \propto \left| \frac{M_{vc}^{(2)} M_{vv}^{(2)}}{-\hbar\omega_2} + \frac{M_{cc}^{(2)} M_{vc}^{(2)}}{\hbar\omega_2} \right|^2 . \qquad (5)$$

If we now consider the case of D-2PA in a direct narrow-gap semiconductor at the pump wavelength (energy of $\hbar\omega_2$), we obtain two terms with the same denominator energy values. Since the momentum matrix elements depend mainly on the symmetry of the bands involved [13], for similar systems (zincblende structures for instance) we should expect values of the same order of magnitude. The difference here, however, is the necessity of having only one long wavelength photon. Also, to obtain the highest nonlinearities it is necessary to probe close to the linear absorption edge, effectively narrowing the available spectral range. To overcome this, a very high quality sample should be used, possibly at a low temperature in order to minimize any linear losses on the probe beam. However, there is an upper limit to the nonlinearities that can be obtained in a nondegenerate configuration. The main limitation is the linear absorption at the probe wavelength below the bandgap, i.e. Urbach tail absorption. Assuming the upper energy limit for the probe photons set to 0.97 of the bandgap energy, by using pump photons at about 5% of the bandgap energy one would theoretically obtain an increase of the 2PA coefficient of only about 2 × versus pumping with photons at 10% of the bandgap. It is important to mention that such enhancements can be obtained in any direct-gap system provided that appropriate photon pairs are used. In systems with strict selection rules

#153971 - $15.00 USD Received 6 Sep 2011; revised 24 Oct 2011; accepted 25 Oct 2011; published 28 Oct 2011

there are additional restrictions which may put an upper practical limit on the measured enhancement [14].

For the highly nondegenerate experiments, the behavior of the Kerr index in particular spectral ranges is also very interesting. The nondegenerate nonlinear index can be obtained using the general expression of the change in absorption caused by the presence of a pump beam and performing a Kramers-Kronig transformation [3,9]. The nonlinear refractive index contains contributions from the 2PA, Raman and Stark processes.

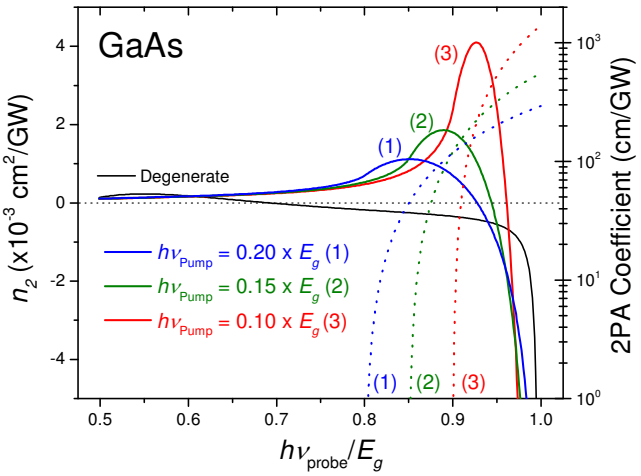

Fig. 5. Calculated nondegenerate induced refraction index (solid lines) and nondegenerate 2PA (dotted lines) of GaAs for pump energies equal to (1) 20% (4.32 μm), (2) 15% (5.81 μm) and (3) 10% (8.84 μm) of the bandgap.

As discussed explicitly in Ref [3], the 2PA terms gives the main contribution, positive for lower energy photons and negative for energies close to the bandgap. The Stark terms give an overall negative contribution to the nonlinear index, which increases asymptotically close to the band edge, while the Raman term adds positively.

For the nondegenerate case, this makes the calculated overall enhancement relatively smaller than for 2PA when using small photon energy pumps. The nonlinear index takes positive values (focusing nonlinearity) for small probe frequencies and turns negative (defocusing nonlinearity) for frequencies close to the 1PA edge. The probe frequency for which the nonlinear index becomes zero depends strongly on the pump frequency. This zero crossing occurs near the peak of the 2PA for the degenerate case approaching frequencies very close to the linear absorption edge as the energy of the pump photons is decreased. The slope of the spectrum near the zero crossing point also changes strongly with the pump photons' energy and becomes extremely steep for small energy pump photons. This leads to changes in the sign of the refractive nonlinearity over very narrow spectral ranges. These trends are shown in Fig. 5 for the particular case of GaAs.

When pumping at ~10% of the bandgap (8.84 μm), by varying the probe wavelength by ~13 nm, from 903 nm to 916 nm, we can vary the n_2 from -2×10^{-12} cm^2/W to 2×10^{-12} cm^2/W, numbers that in absolute value correspond to about 50% of the peak n_2. To verify this, picosecond pulses would be more suitable because of their narrower spectral widths; however, it would also be interesting to study the effect of this spectral dependence on a femtosecond pulse with a large bandwidth centered near the zero crossing frequency. Unfortunately, from the standpoint of applications, the nonlinear refraction is largely enhanced in spectral regions where the 2PA is also enhanced, see Fig. 5. To minimize losses, future applications would require avoiding these enhanced 2PA ranges, making use of only moderate enhancements in nonlinear refraction and the judicious choice of direct-gap semiconductor.

#153971 - $15.00 USD Received 6 Sep 2011; revised 24 Oct 2011; accepted 25 Oct 2011; published 28 Oct 2011

5. Conclusions

We measure nondegenerate 2PA spectra of several semiconductors (CdTe, GaAs, ZnS, ZnSe, and ZnO) using pairs of extremely nondegenerate photons. The magnitude of the 2PA coefficients increases dramatically when low energy pump photons, compared to the bandgap energy, are used. Very good agreement with calculations based on the "dressed" wavefunctions approach is shown. For our experiments in ZnSe, the measured non-degenerate 2PA is as large as 270 × the corresponding degenerate 2PA value when pumping with low energy photons of 0.08 E_g. This corresponds to a 50 × increase over the peak degenerate 2PA coefficient. Using even lower photon energies is theoretically predicted to lead to larger enhancements. The large nonlinearities measured, minimization of free-carrier effects, and the possibility to tailor the Kerr index behavior by the appropriate choice of wavelengths, suggest that efficient all-optical switching may be implemented [26]. These large enhancements made possible the demonstration of gated detection in a room temperature GaN photodiode with very good sensitivity [6]. This large enhancement of the 2PA coefficient also translates directly to enhanced two-photon gain [27], which opens the possibility of highly nondegenerate two-photon tunable laser and amplifier device applications [8]. However, it remains to be seen if the strong enhancement in two-photon emission would be sufficient to overcome the large free-carrier losses of the infrared wave in such devices.

Acknowledgements

This work was supported in part by the US Army Research Office (grant no. 50372-CHMUR) and the DARPA ZOE program (grant no. W31R4Q-09-1-0012).

#153971 - $15.00 USD Received 6 Sep 2011; revised 24 Oct 2011; accepted 25 Oct 2011; published 28 Oct 2011